Two novel halogeno(cyano)argentates built by silver halide clusters: molecular structures and luminescent properties

Ying-Bing Lu,[ab] Li-Zhen Cai,[a] Jian-Ping Zou,[a] Xi Liu,[a] Guo-Cong Guo,[* a] and Jin-Shun Huang[a]

[a]*State Key Laboratory of Structural Chemistry, Fujian Institute of Research on the Structure of Matter, Chinese Academy of Sciences, Fuzhou, Fujian 350002, P. R. China. Fax: 86 591 83714946. E-mail:* gcguo@fjirsm.ac.cn.

[b]*College of Chemistry and Life Science, Gannan Normal University, Ganzhou, 341000, P. R. China.*

Theoretical Approach Methodology. The electronic ground states of the two complexes were calculated by using B3LYP density functional theory. 3-21G quality basis sets were employed for all atoms. The ground state geometry was adapted from the truncated X-ray data, $[Ag_{12}(CN)_{11}Br_{10}]^{9-}$ for **1** and $[Ag_{12}(CN)_{11}I_{10}]^{9-}$ for **2**. Based on these geometries, time-dependent DFT (TDDFT) calculation using the B3LYP functional was carried out. The ground-state B3LYP and excited-state TDDFT calculations were carried out using Gaussian2003.[i] More accurate data could be obtained with more sophisticated theoretical approaches to gain detailed insights into the energy correlation among various electronic states for nontruncated structures.
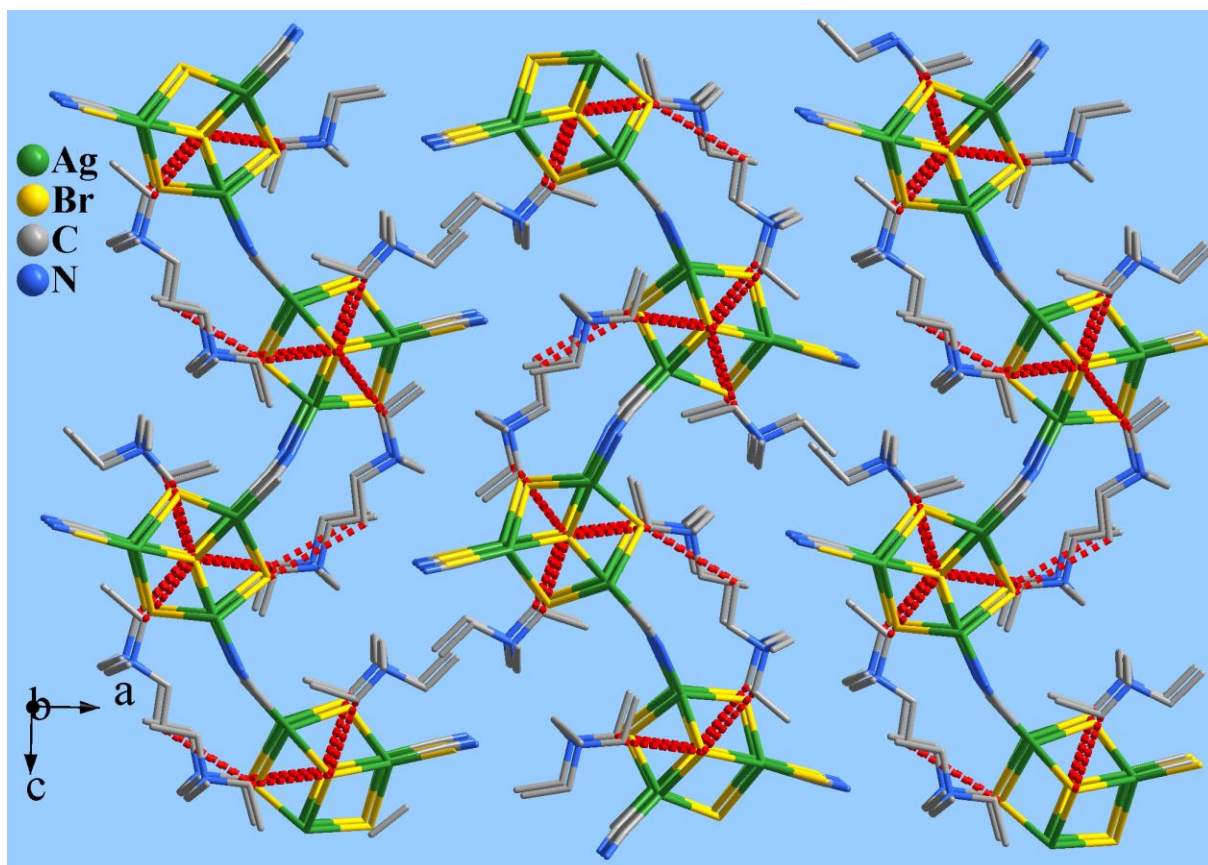
Figure S1. Crystal structure of **1** viewing along the *b* axis showing the [Et$_4$N]$^+$ cations being located between the layers. The red dash lines represent the C-H…Br H-bonds.
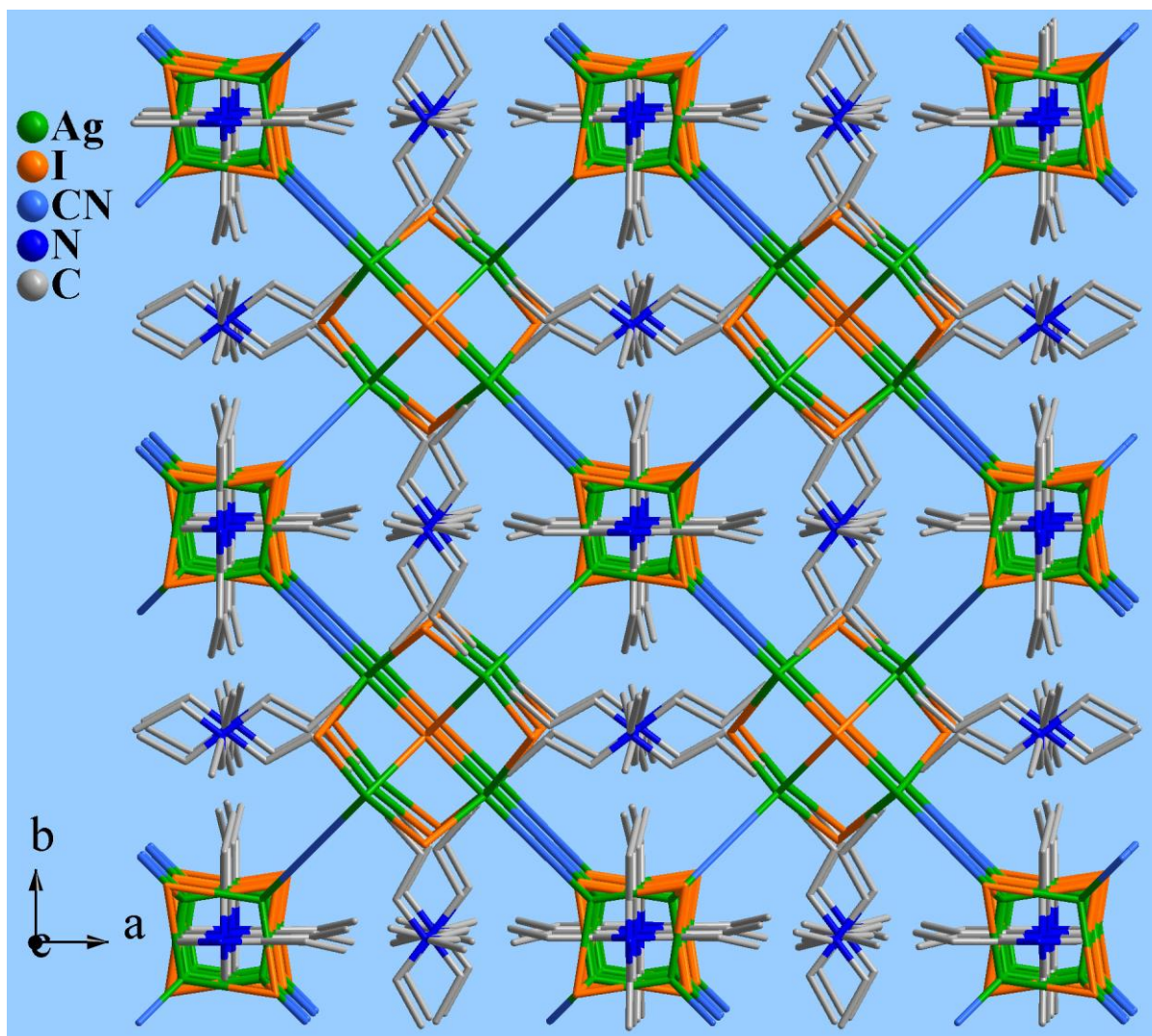
Figure S2. 3-D network of **2** viewing along the *c* axis with the $(Pp_4N)^+$ cations locating the channels.
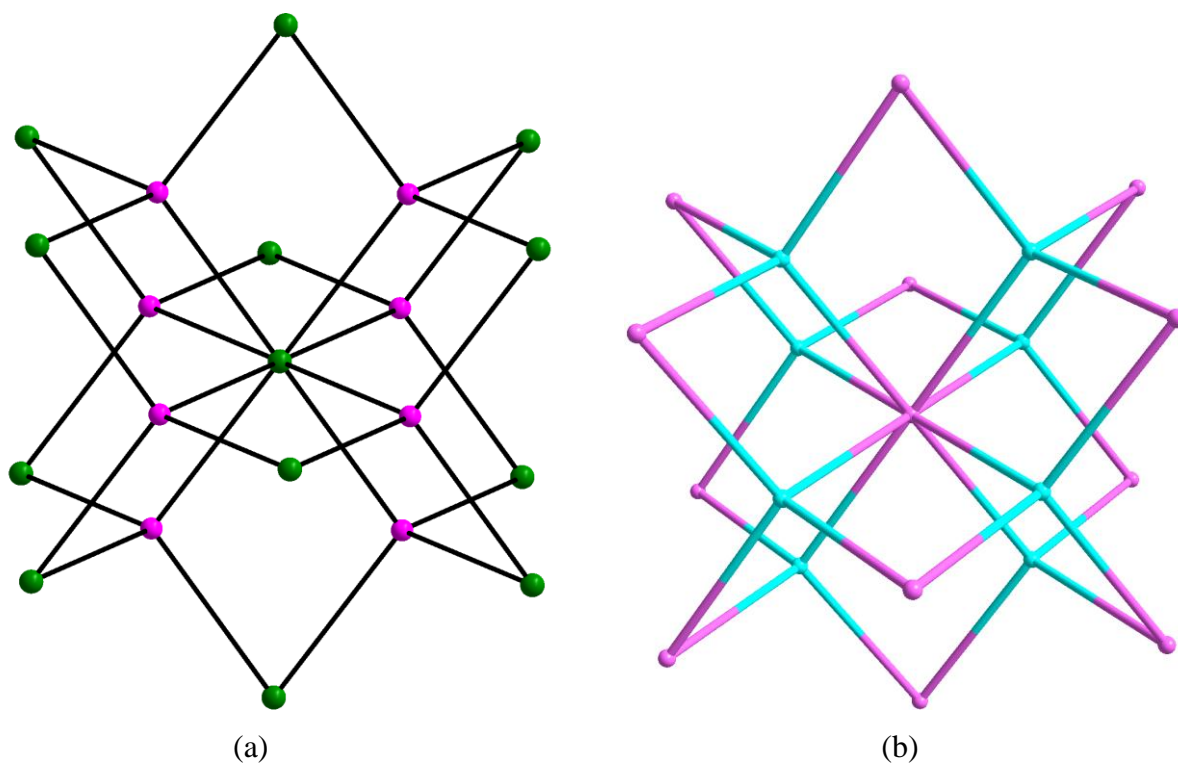
(a)

(b)

Figure S3. (a) Fluorite topology of **2** (green for octanuclear clusters, red for tetranuclear clusters); (b) CaF$_2$ structure (pale red for Ca ions, pale blue for F ions).
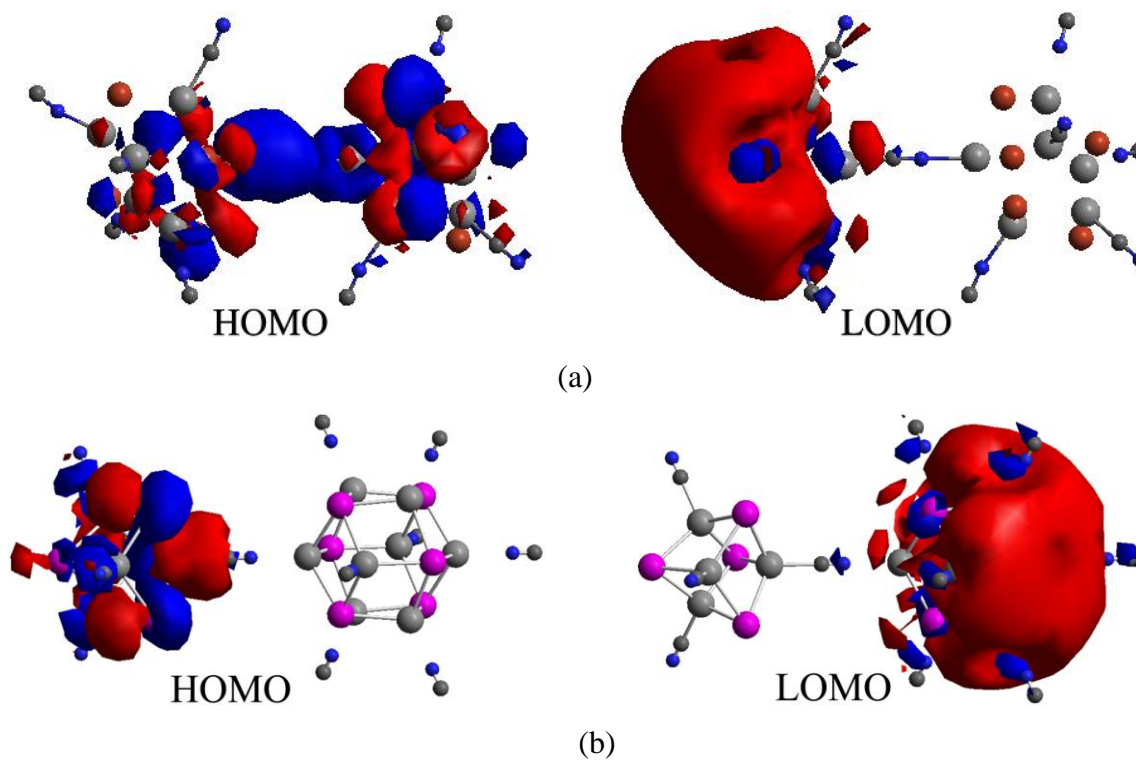

HOMO

LOMO

(a)

HOMO

LOMO

(b)

Figure S4. Electron-density distribution of the lowest unoccupied and highest occupied frontier orbitals calculated for **1** (a) and **2** (b).

Table S1. The C–H···Br hydrogen bonds in **1**.

D–H···A	D–H···A (Å)	∠(DHA) (°)
C14–H14A···Br1	3.807	174.9
C15–H15A···Br4	3.744	147.0
C24–H24A···Br2	3.943	169.7
C25–H25A···Br4	3.831	139.7
C32–H32A···Br4	3.772	147.8

Table S2. The calculated excitation (E), energy, oscillator strength (f), and dominant orbital excitation from TD-DFT calculations for the lowest singlet excitation states.

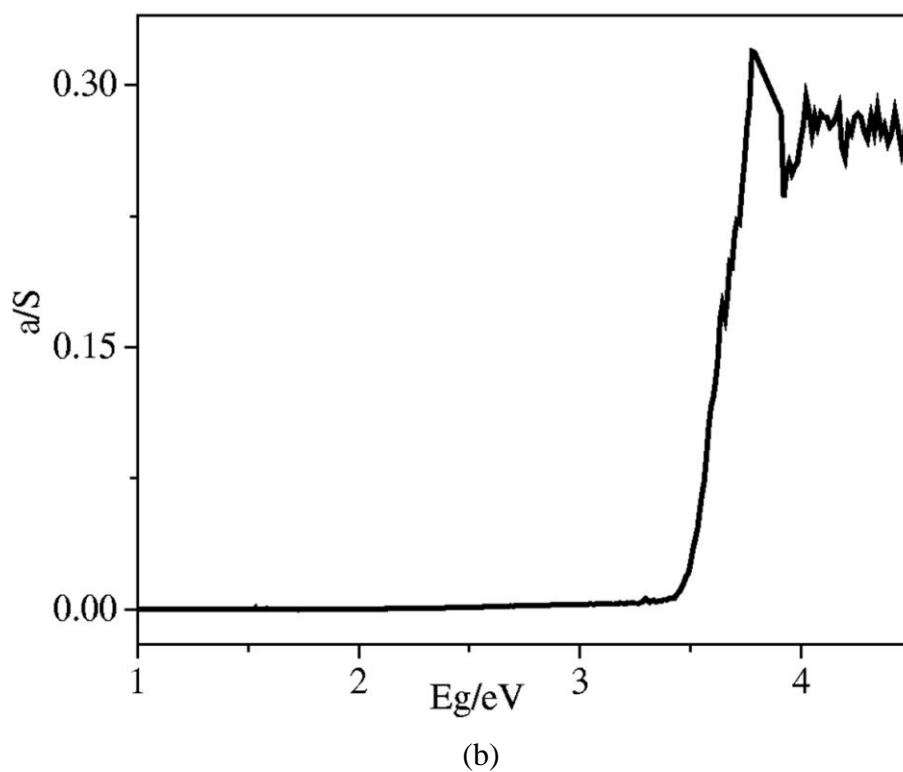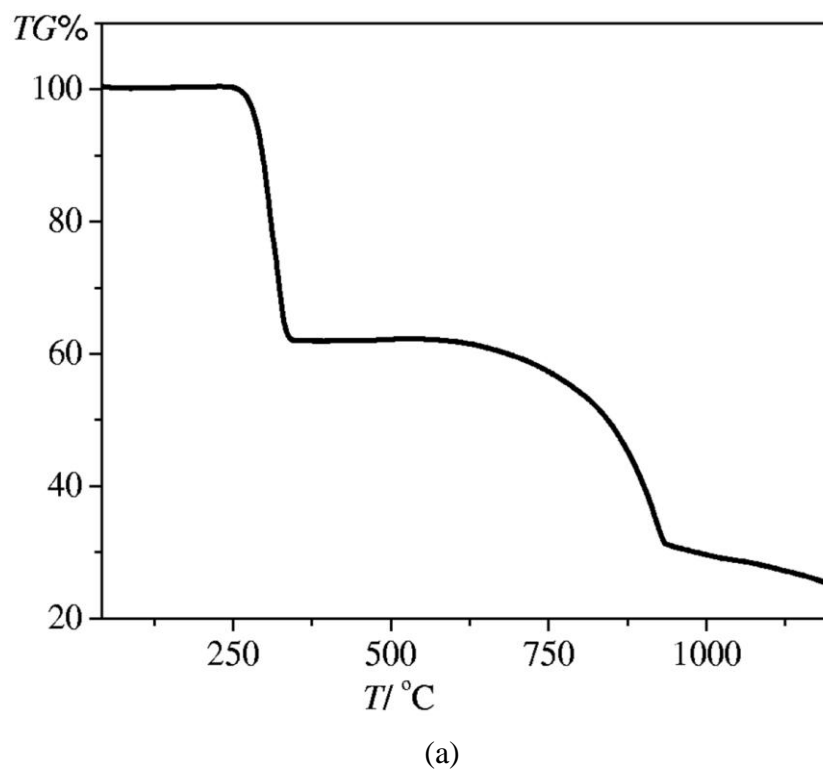| Complexes	Ex (nm)	Energy (eV)	f	Dominant configurations
1	315.8	3.93	0.0446	HOMO → LUMO
2	356.0	3.48	0.0023	HOMO → LUMO

(a)

(b)
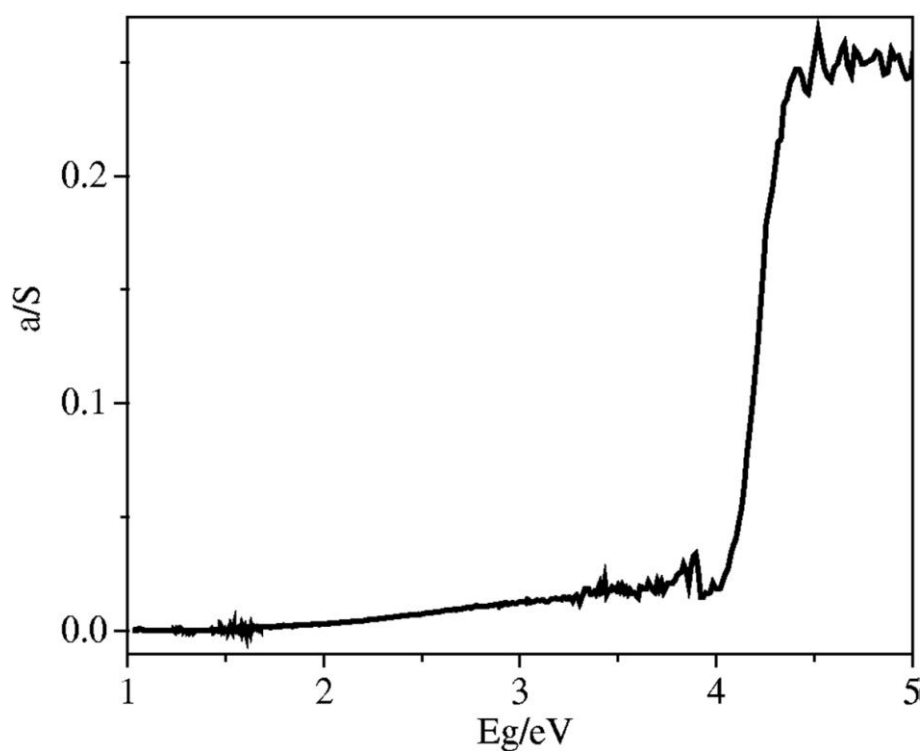
Figure S5. Optical absorption spectra for **1** (a) and **2** (b).
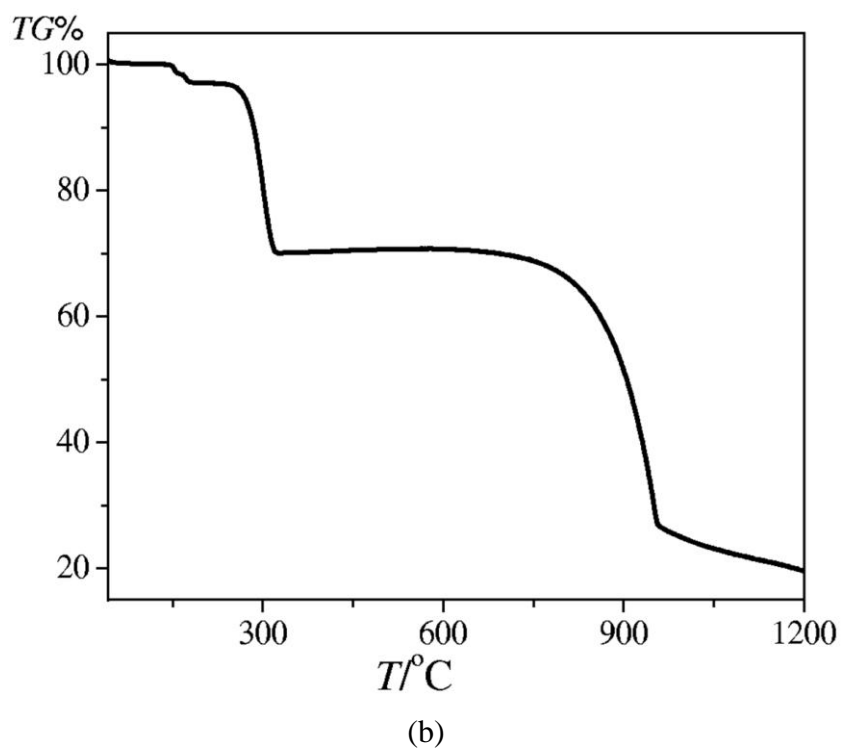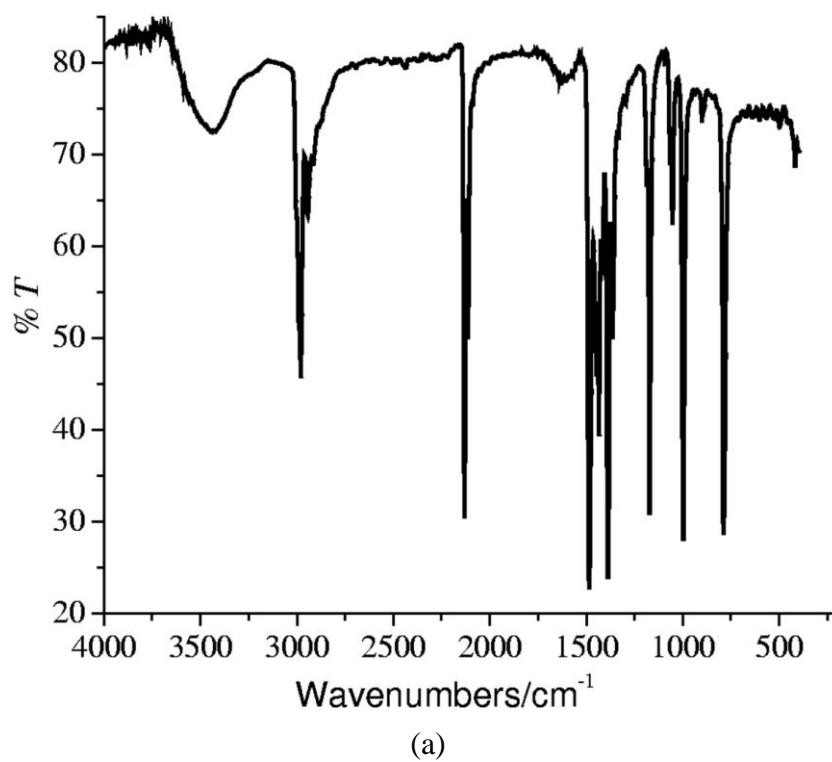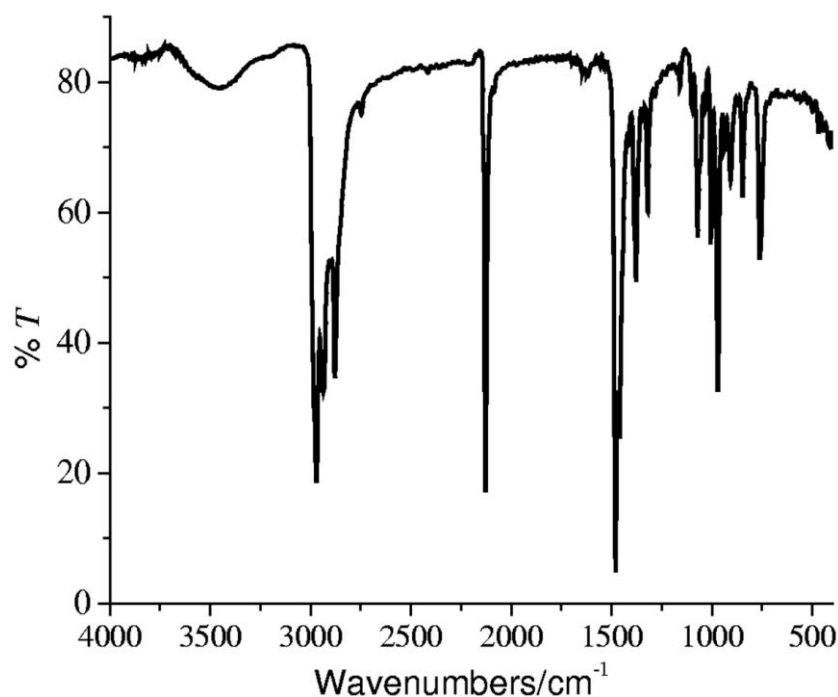

(a)

(b)

Figure S6. Thermogravimetric analysis curves for **1** (a) and **2** (b).

(a)

7

(b)

Figure S7. IR spectra for **1** (a) and **2** (b).

i   Gaussian 03, Revision B.02, M. J. Frisch, G. W. Trucks, H. B. Schlegel, G. E. Scuseria, M. A. Robb, J. R. Cheeseman, J. A. Montgomery, Jr., T. Vreven, K. N. Kudin, J. C. Burant, J. M. Millam, S. S. Iyengar, J. Tomasi, V. Barone, B. Mennucci, M. Cossi, G. Scalmani, N. Rega, G. A. Petersson, H. Nakatsuji, M. Hada, M. Ehara, K. Toyota, R. Fukuda, J. Hasegawa, M. Ishida, T. Nakajima, Y. Honda, O. Kitao, H. Nakai, M. Klene, X. Li, J. E. Knox, H. P. Hratchian, J. B. Cross, C. Adamo, J. Jaramillo, R. Gomperts, R. E. Stratmann, O. Yazyev, A. J. Austin, R. Cammi, C. Pomelli, J. W. Ochterski, P. Y. Ayala, K. Morokuma, G. A. Voth, P. Salvador, J. J. Dannenberg, V. G. Zakrzewski, S. Dapprich, A. D. Daniels, M. C. Strain, O. Farkas, D. K. Malick, A. D. Rabuck, K. Raghavachari, J. B. Foresman, J. V. Ortiz, Q. Cui, A. G. Baboul, S. Clifford, J. Cioslowski, B. B. Stefanov, G. Liu, A. Liashenko, P. Piskorz, I. Komaromi, R. L. Martin, D. J. Fox, T. Keith, M. A. Al-Laham, C. Y. Peng, A. Nanayakkara, M. Challacombe, P. M. W. Gill, B. Johnson, W. Chen, M. W. Wong, C. Gonzalez, and J. A. Pople, Gaussian, Inc., Pittsburgh PA, 2003.